Transport in insulating $YBa_2Cu_3O_{7-\delta}$

F. P. Milliken, T. Doderer,* R. H. Koch, and C. C. Tsuei
IBM Thomas J. Watson Research Center, Yorktown Heights, New York 10598
(Received 29 November 1999; revised manuscript received 22 March 2000)

We have measured the transport properties in field effect transistors that incorporate underdoped $YBa_2Cu_3O_{7-\delta}$ as the conducting channel material. Once fabricated, devices are deoxygenated in argon gas at temperatures 250–350 °C. The devices are then vapor cooled above a bath of liquid helium and two-wire resistivity measurements are made between room temperature and 4.2 K. For zero applied gate voltage (V_g) and in sufficiently underdoped devices we observe two-dimensional (2D) Mott variable range hopping (VRH). As we remove more oxygen, we observe a transition to Efros-Shklovskii VRH. For $V_g<0$ we generally observe 2D Mott VRH.

There have been several recent papers reporting efforts to make non-silicon-based field effect transistors (FET's) using a cuprate material for the conducting channel. These efforts usually take one of two standard approaches. One approach is to make superconducting FET's that are operated below the superconducting transition temperature of the cuprate.[1–5] An alternative approach is to use an underdoped or ''insulating'' cuprate and operate the device at room temperature.[6–11] These technologies are interesting since they are not expected to have the same scaling limitations inherent in Si FET technology.[6,7]

Typical insulating FET devices are fabricated starting with fully oxygenated high-T_c cuprate material. The devices are then made insulating by removing some amount of oxygen. Often, it is the case that the term ''insulating'' is loosely used and it is not in fact known precisely what type of insulating transport is occurring in the cuprate channel. Furthermore, the nature of the transport may change as we change the number of carriers using an applied gate voltage (V_g). There are several characteristic temperature dependences for insulating transport. The simplist type of insulator is an intrinsic semiconductor at low temperatures. In this case the resistivity is simply activated, i.e., $\rho \sim \exp(E_g/k_BT)$, where E_g is the gap energy and k_B is Boltzmann's constant. However, in insulating cuprates the most commonly observed type of transport is Mott variable range hopping.[12] Variable range hopping (VRH) is observed at low temperatures in systems where there are a finite number of localized states at the Fermi energy. The resistivity is then given by

$$\rho(T)=\rho_0 \exp[(T_0/T)^{1/(d+1)}], \tag{1}$$

where d is the relevant dimensionality of the system, T_0 is a parameter that depends on the localization length and the density of states at the Fermi energy, and ρ_0 is a temperature independent constant at very low temperatures. The parameter T_0 is determined by fitting Eq. (1) to measurements of ρ vs T. If the carrier density is sufficiently low, screening becomes less effective and electron-electron interactions are then important. This results in a soft or Coulomb gap at the Fermi level and Efros-Shklovskii (ES) VRH are observed.[13] The temperature dependence in this case is

$$\rho(T)=\rho_0 \exp[(T_0^{\mathrm{ES}}/T)^{1/2}], \tag{2}$$

where the parameter T_0^{ES} is again determined by measurements. We note that Eq. (2) does not depend on the dimensionality d.

In underdoped cuprates VRH has been observed by many groups. Unfortunately, the observed temperature dependences are not usually well defined. VRH has been most cleanly identified in bar shaped poly- crystalline $La_{2-x}Sr_xCuO_4$,[14] in single crystals of $Y_{1-x}Pr_xBa_2Cu_3O_{7-\delta}$,[15] and in single crystals of $La_{2-y}Sr_yCu_{1-x}Li_xO_{4-\delta}$.[16] In this paper we present our measurements of ρ vs T for several insulating FET devices. For the conducting channel we use $YBa_2Cu_3O_{7-\delta}$ (YBCO) or $Y_{0.5}Pr_{0.5}Ba_2Cu_3O_{7-\delta}$ (YPBCO) material. Our goal is to identify the relevant transport mechanism occurring in these devices as we change the number of carriers either chemically by removing oxygen or electronically by changing V_g. For $V_g=0$ and in sufficiently deoxygenated devices we observe two-dimensional (2D) Mott VRH. As we remove more oxygen we observe ES VRH. For $V_g<0$ we again observe 2D Mott VRH.

A schematic drawing of one of our FET devices is shown in Fig. 1. The substrate is single-crystal electrically conducting Nb-doped $SrTiO_3$ and is used as the gate (G). A 400 nm layer of undoped STO is then deposited on top of G. This is followed by a 50 nm layer of c-axis oriented YBCO (or YPBCO) grown epitaxially on top of the STO layer. The device is completed by adding platinum source (S) and drain (D) electrodes. Finally, we isolate the individual devices on a given chip by cutting trenches with a patterned laser beam. A single FET device typically has a channel length $l=5\ \mu$m and width $w=90\ \mu$m. The large source and drain electrodes

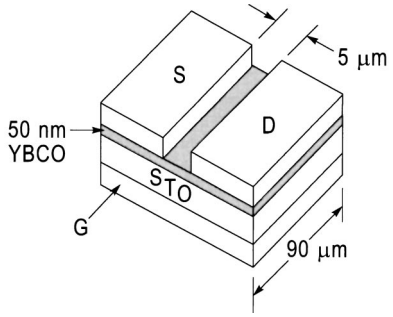

FIG. 1. Schematic drawing of FET with YBCO material for the conducting channel.

TABLE I. Final annealing parameters and starting resistivities at 290 K for eight devices. T_0 and T_0^{ES} are obtained by fitting Eqs. (1) or (2) to measurements of ρ vs T with $V_g=0$.

Device	Material	Final anneal in Ar	ρ(290 K) (Ω cm)	T_0 or T_0^{ES} (K)	
1 (343*d*)	YPBCO		1.08×10^3	4.6×10^4	ES
2 (425*h*)	YPBCO	1/4 h @ 250 °C	1.66	5100	ES
3 (425*i*)	YPBCO	same	2.2		
4 (471*m*)	YBCO	1h @ 310 °C	16.1	640	ES
5 (471*r*)	YBCO	1h @ 320 °C	6.6×10^5	3.8×10^5	ES
6 (471*u*)	YBCO	1h @ 290 °C	0.30	430	Mott 2D
7 (450*d*)	YBCO	1h @ 310 °C	760		
8 (450*f*)	YBCO	same	67		

help minimize any possible contact resistance problems. Additional fabrication details may be found elsewhere.[7,8]

Each chip starts out with fully oxygenated YBCO. Oxygen is then removed from the chip through controlled annealing in Ar at a temperature of 250–350 °C for 1–2 h. The precise amount of oxygen removed (δ) is not known, but, if necessary, we could estimate δ from the measured resistivity at room temperature.[17,18] We note that YBCO begins to show ''insulating'' behavior for δ greater than about 0.5. Removing oxygen effects the conducting channel in two ways: (1) it reduces the number of carriers (holes) and (2) it introduces disorder. A list of the final annealing parameters for each device studied is given in column 3 in Table I. In column 1 the label in parentheses gives the three-digit chip number and the individual device letter. The fourth column gives the starting resistivity of each device at 290 K. The last column gives values for T_0 or T_0^{ES} obtained by fitting Eqs. (1) or (2) to measurements of ρ vs T. Entries that are left blank usually imply that there are not enough low T data to reliably determine T_0 or T_0^{ES}.

The devices are vapor cooled above a bath of liquid helium and the temperature T is measured using a Si-diode thermometer. Two-wire dc resistance measurements are obtained using a battery powered power supply and a low noise current preamp. The sample resistance R is calculated differentially:

$$R=\Delta V_{SD}/\Delta I_{SD}=[V_{SD}-V_{SD}(0)]/[I_{SD}-I_{SD}(0)],$$

where V_{SD} is the applied source-drain voltage, I_{SD} is the source-drain current, $V_{SD}(0)$ is the voltage across the device for zero applied voltage, and $I_{SD}(0)$ is the corresponding ''zero bias'' current. The applied voltage is always chosen such that we are in an Ohmic regime and in practice we usually operate at voltages less than 10 mV. The highest resistance that we can reliably measure with our setup is about 200 GΩ. The resistivity ρ is calculated using the 3D formula $\rho=(dw/l)R$ where d is the thickness of the YBCO film. For most of our devices $d=50$ nm. This gives $(dw/l)=900$ nm. In the literature most measurements of the resistivity of YBCO assume 3D transport. Clearly this is appropriate in polycrystalline material; however, this is not necessarily appropriate for our epitaxially grown thin films. Since the resistivity in the *c*-axis direction is much larger than in the *ab* plane,[19] it may be more suitable to calculate the 2D resistivity or $R_\square$. In this case $\rho(2D)=R_\square\simeq(500/11.68)(w/l)\times R\simeq771\times R$, where the factor (500/11.86) is just the number of layers conducting in parallel. Despite these considerations, in this paper ρ will be given in Ω cm units in order to be consistent with published numbers. None of the conclusions drawn in this paper are affected by this choice.

We shall now consider our measurements for the case $V_g=0$. In Fig. 2(a) we plot the log of the resistivity of three devices vs $T^{-1/3}$. This is the expected temperature dependence for conventional 2D Mott VRH [Eq. (1) with $d=2$]. The straight lines are guides for the eye. Each device has a different amount of oxygen removed as indicated in Table I. Overall, we see that for fixed temperature T the resistivity ρ increases as we remove more oxygen. Also, as expected, the temperature dependence is stronger in devices that are more deoxygenated. Let us then discuss each device shown starting with device 6.

We see that device 6 seems to obey the $T^{-1/3}$ temperature dependence quite well.[20] If we fit Eq. (1) with $d=2$ to the data shown in Fig. 2(a) we get $T_0=430$ K. The data for device 6 span almost two decades in T and therefore give fairly convincing evidence that the relevant transport picture is indeed 2D Mott VRH. In this case we can calculate the localization length ξ using the formula $k_BT_0=\beta/N(E_F)\xi^2d$, where $\beta\simeq3$ (Ref. 12) and $N(E_F)$ is the 3D density of states at the Fermi energy. Ordinarily, since the *S* and *D* pads sit on top of the YBCO and since the resistivity in YBCO is very anisotropic, we might assume that the main conduction path is along a single layer next to the *S* and *D* pads and therefore the relevant d would be 12 Å. However, since the YBCO layer is fairly thin we would expect many defects, in particular grain boundaries. Thus, given that the pads are relatively large, we feel that carriers will be able to tunnel to all layers and therefore the relevant d is the thickness of the YBCO film. We do not of course know $N(E_F)$ precisely. This will depend on how much oxygen has been removed and other sample specific details. We estimate $N(E_F)$ using the following argument. We assume that for $V_g=0$, E_F in our underdoped samples lies somewhere between lower and upper Hubbard-like bands.[8] Calculations[21] show that $N(E)\simeq1$ state/eV cell near the edge of the lower band in YBCO. It is reasonable that $N(E_F)$ will be somewhat lower and therefore we choose $N(E_F)=0.3$ states/eV cell. If $T_0=430$ K and $d=50$ nm, we then calculate $\xi\simeq10$ Å.

Device 4 exhibits a stronger T dependence and overall clearly does not obey a $T^{-1/3}$ temperature dependence. In

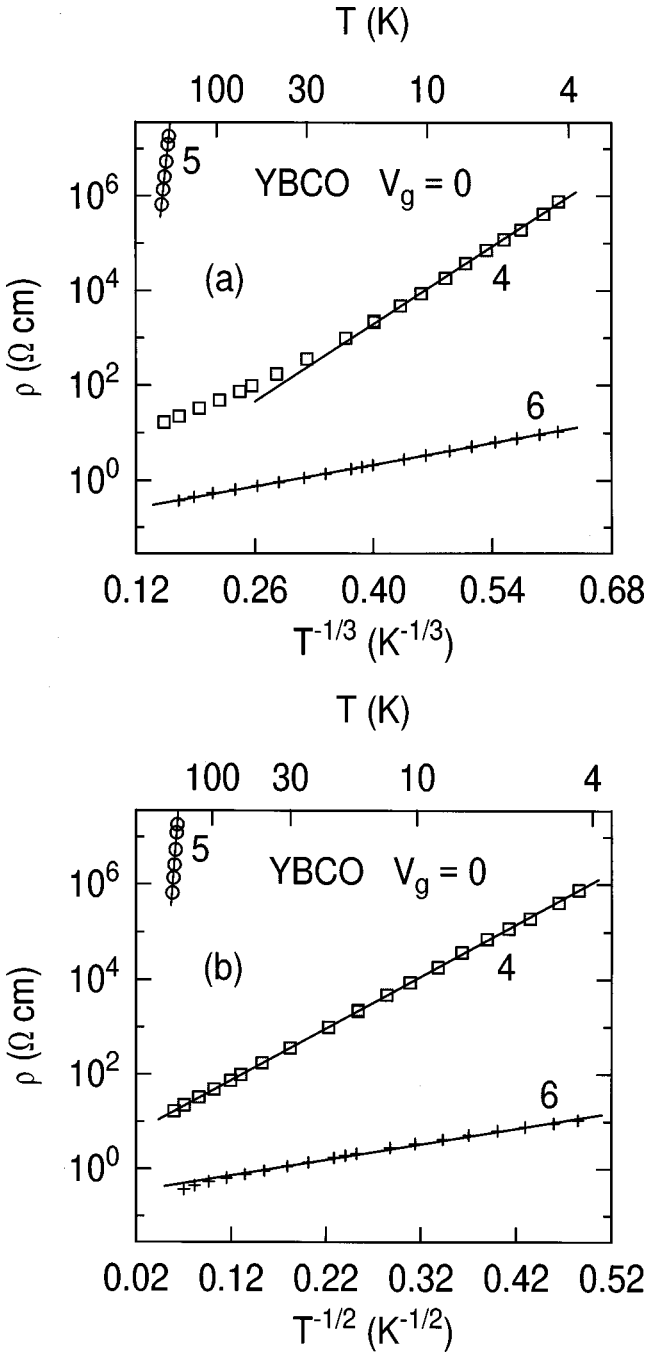

FIG. 2. (a) Resistivity vs $T^{-1/3}$ for three devices made with YBCO. All devices are on the same chip and each device has a different amount of oxygen removed. (b) Resistivity vs $T^{-1/2}$ for the same data shown in (a). The lines are guides for the eye.

fact, careful inspection of the line drawn through the low T data shows that the data are still curving upwards and therefore even at low temperatures the $T^{-1/3}$ dependence is not appropriate. We shall consider another possible T dependence for this data in a moment. Finally, let us consider device 5. The T dependence is extremely strong and we very quickly go beyond the resistance range that we can measure. Given the limited range in R, we can easily draw a straight line through this data. However, the T dependence is not in fact uniquely determined and therefore nor is the relevant transport mechanism.

In Fig. 2(b) we replot the same data shown in Fig. 2(a) but vs $T^{-1/2}$. Figure 2(b) shows that $T^{-1/2}$ is too fast for device 6 but now gives a very good fit to the data for device 4. The fit for device 4 is exceptionally good. Here, T changes by almost two orders of magnitude while ρ changes by almost five orders of magnitude. If we fit Eq. (2) to the data for device 4 we get $T_0^{ES}=640\,K$. We recall that a $T^{-1/2}$ dependence is expected for both simple 1D Mott VRH and ES VRH. For ES VRH,[13] $k_B T_0^{ES} \simeq e^2/\kappa\xi$, where in YBCO the dielectric constant $\kappa \simeq 25$.[1] If $T_0^{ES}=640\,K$, we calculate $\xi \simeq 10\,Å$. This number is obtained without any knowledge or assumptions regarding $N(E_F)$. For 1D Mott VRH,[13] $k_B T_0 \simeq 1/N(E_F)\xi dw$. If we assume $N(E_F)=0.3$ states/eV cell and if $T_0=640\,K$, we find $\xi \simeq 3\times 10^{-5}\,Å$, which is not reasonable. In conclusion, it must be the case that the overlap of the quantum-mechanical wave functions of the localized states near E_F is too small to permit adequate screening of *e-e* interactions and therefore the $T^{-1/2}$ dependence predicted by Efros-Shklovskii is exhibited. The transition shown in Fig. 2 from 2D Mott VRH to ES VRH, which results as we remove oxygen, has not been cleanly observed before. A similar transition has been observed in doped $La_{2-x}Sr_xCuO_4$ samples as the amount of Sr is varied.[14] In contrast to these earlier studies, the transition that we observe is seen in a single (made only once) chip.

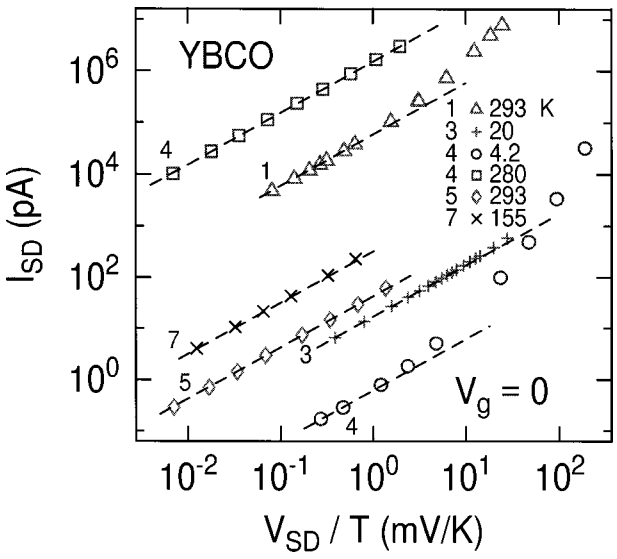

FIG. 3. Current vs voltage for several devices at different fixed temperatures.

In Fig. 3 we plot I_{SD} vs V_{SD} data for five of our devices at various fixed temperatures. Here V_{SD} is the applied bias and I_{SD} is the measured current. Each data point has been rescaled by dividing the applied bias by the temperature T at which V_{SD} and I_{SD} are measured. The straight dashed lines are guides to the eye and indicate the expected linear dependence of I_{SD} on V_{SD} in the Ohmic regime. We see that we remain in the Ohmic regime as long as V_{SD}/T is less than about 1 mV/K. We would like to emphasize that all measurements shown in Fig. 2 were taken under ''Ohmic'' conditions. Contact resistance issues are always a concern when doing two-wire measurements and therefore insuring that we are always in an Ohmic regime is essential. We note that if we use sufficiently large applied voltages we move beyond the Ohmic regime and we then observe heating effects which

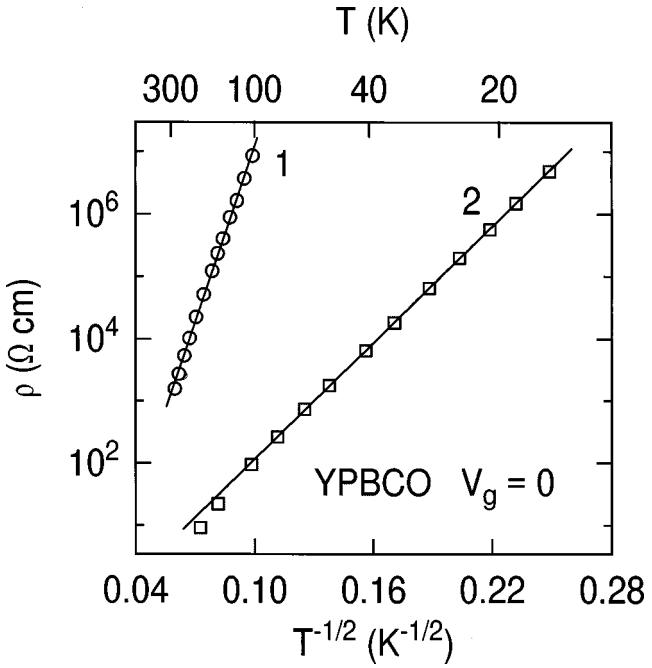

FIG. 4. Resistivity vs $T^{-1/2}$ for two devices made with YPBCO.

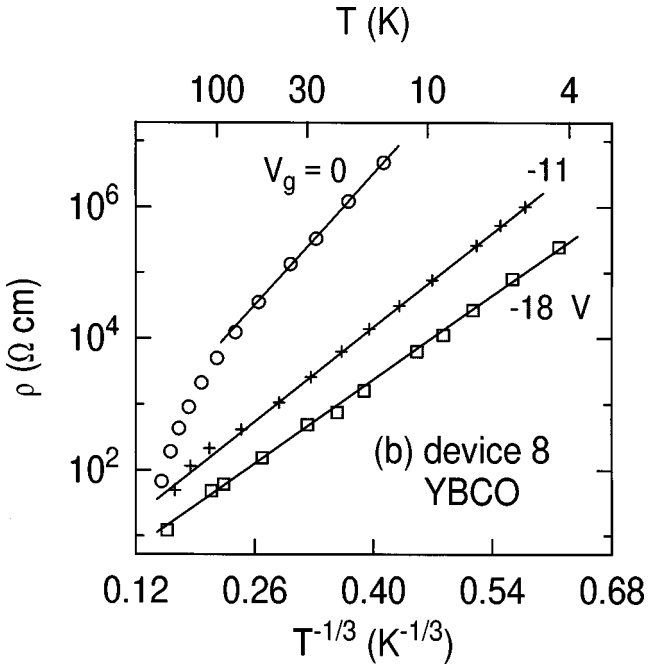

FIG. 5. Resistivity vs $T^{-1/3}$ for device 8 for several applied gate voltages.

result in the flattening of our $\rho(T)$ curves at low temperatures. This of course is to be avoided.

So far we have discussed only YBCO devices. We also have early YPBCO data that are shown in Fig. 4. We note that devices 1 and 2 are not on the same chip (see Table I). Device 2 apparently already has had sufficient oxygen removed that Efros-Shklovskii transport is observed. After a temporary high-temperature correction, convincing $T^{-1/2}$ behavior is observed for more than five decades in ρ. If we fit Eq. (2) to the data for device 2 we obtain $T_0^{\mathrm{ES}}=5100\,\mathrm{K}$. Device 1 also shows a weak high-temperature correction and, given the limited amount of low T data, the temperature dependence is not well defined. High-temperature corrections are often observed in insulating samples[13] and frequently are device specific. In this paper we generally weigh more heavily measurements at lower temperatures where these effects are less important. In summary, the main point shown in Fig. 4 is that ES behavior is commonly observed in our devices.

All data presented so far were taken with $V_g=0$. We shall now consider what happens when $V_g\neq 0$. In Fig. 5 we show data for device 8 for three different gate voltages. The straight lines are guides for the eye. For $V_g=0$ we observe significant high-temperature effects which complicate our ability to uniquely determine the relevant temperature dependence. However, since the starting resistivity is fairly high, we would expect ES VRH at the lowest temperatures. The most interesting feature shown in Fig. 5 is that for $V_g=-11$ and -18 V the data clearly follow a $T^{-1/3}$ temperature dependence. The T_0's are 1.86×10^4 K and 9.1×10^3 K for $V_g=-11$ and -18 V. For $V_g>0$ the resistivity increases a small amount with respect to the $V_g=0$ data (not shown). We interpret the observed $T^{-1/3}$ temperature dependence for $V_g<0$ in the following way. As we make V_g negative we add holes to the cuprate material next to the YBCO/STO interface. The thickness of this layer is given by the Thomas-Fermi screening length and is estimated to be about 1 nm.[8] The holes added are not very mobile but they provide additional hopping sites for carriers in this layer. These additional sites must allow significant wave function overlap and therefore interactions in this layer are effectively screened. Thus the main transport mechanism in this layer is 2D Mott VRH. Finally, since this layer is much more conducting than the other layers this layer dominates the overall T dependence of the device.

We have considered one other possible interpretation for the apparent $T^{-1/3}$ behavior observed for $V_g<0$. It is possible that *e-e* interactions in the layer next to the STO are still important and the relevant transport in this layer is still ES VRH. In this case the temperature dependence of this layer is $T^{-1/2}$. This ''surface'' layer then conducts in parallel with the remaining more resistive ''bulk'' layer. The temperature dependence of the bulk layer is given by the $V_g=0$ data shown in Fig. 5. If we combine the conductance of these two layers we can try to fit the $V_g<0$ data shown in Fig. 5. When we do this the fit to the data is not as good as the simpler $T^{-1/3}$ fit shown in Fig. 5, and therefore it is unlikely that ES VRH is occurring in the surface layer next to the STO.

In summary, we have investigated the transport properties of several FET devices where the conducting channel material is deoxygenated YBCO. We find that in sufficiently deoxygenated devices and for $V_g=0$ we observe 2D Mott VRH. As we remove more oxygen, we observe a transition to transport that is dominated by *e-e* interactions. In this case ES VRH is observed. In very insulating devices we observe a return to 2D Mott VRH for $V_g<0$.

We thank J. A. Misewich and D. M. Newns for stimulating discussions and G. Trafas for valuable technical assistance.

*Present address: Institute of Solid State Physics, Friedrich-Schiller-University, Helmholtzweg 5, D-07743 Jena, Germany.
[1] J. Mannhart, Supercond. Sci. Technol. **9**, 49 (1996).
[2] V. Talyansky, S. B. Ogale, I. Takeuchi, C. Doughty, and T. Venkatesan, Phys. Rev. B **53**, 14 575 (1996).
[3] T. Kawahara, T. Suzuki, E. Komai, K. Nakazawa, T. Terashima, and Y. Bando, Physica C **266**, 149 (1996).
[4] S. Hontsu, H. Tabata, M. Nakamori, J. Ishii, and T. Kawai, Jpn. J. Appl. Phys., Part 2 **35**, L774 (1996).
[5] T. Saito, X. Cai, K. Usami, T. Kobayashi, and T. Goto, IEEE Trans. Appl. Supercond. **7**, 3528 (1997).
[6] C. Zhou, D. M. Newns, J. A. Misewich, and P. C. Pattnaik, Appl. Phys. Lett. **70**, 598 (1997).
[7] D. M. Newns, J. A. Misewich, C. C. Tsuei, A. Gupta, B. A. Scott, and A. Schrott, Appl. Phys. Lett. **73**, 780 (1998).
[8] T. Doderer, C. C. Tsuei, W. Hwang, and D. M. Newns, Phys. Rev. B **62**, 5984 (2000).
[9] A. Levy, J. P. Falck, and M. A. Kastner, W. J. Gallagher, A. Gupta, and A. W. Kleinsasser, J. Appl. Phys. **69**, 4439 (1991).
[10] R. Sobolewski, W. Xiong, and W. Kula, Appl. Phys. Lett. **64**, 643 (1994).
[11] A. Levy, J. P. Falck, M. A. Kastner, R. J. Birgeneau, and A. T. Fiory, Phys. Rev. B **51**, 648 (1995).
[12] N. F. Mott and E. A. Davis, *Electronic Processes in Non-Crystalline Materials*, 2nd ed. (Oxford University Press, London, 1979).
[13] B. I. Shklovskii and A. L. Efros, *Electronic Properties of Doped Semiconductors* (Springer-Verlag, New York, 1984).
[14] B. Ellman, H. M. Jaeger, D. P. Katz, T. F. Rosenbaum, A. S. Cooper, and G. P. Espinosa, Phys. Rev. B **39**, 9012 (1989).
[15] G. A. Levin, T. Stein, C. C. Almasan, S. H. Han, D. A. Gajewski, and M. B. Maple, Phys. Rev. Lett. **80**, 841 (1998).
[16] M. A. Kastner, R. J. Birgeneau, C. Y. Chen, Y. M. Chiang, D. R. Gabbe, H. P. Jenssen, T. Junk, C. J. Peters, P. J. Picone, T. Thio, T. R. Thurston, and H. L. Tuller, Phys. Rev. B **37**, 111 (1988).
[17] H. Takagi, S. Uchida, H. Iwabuchi, H. Eisaki, K. Kishio, K. Kitazawa, K. Fueki, and S. Tanaka, Physica B **143**, 349 (1987).
[18] B. Wuyts, V. V. Moshchalkov, and Y. Bruynseraede, Phys. Rev. B **53**, 9418 (1996).
[19] K. Takenaka, K. Mizuhashi, H. Takagi, and S. Uchida, Phys. Rev. B **50**, 6534 (1994).
[20] We have studied devices that are less deoxygenated and have lower starting resistivities than device 6. In these cases the temperature dependence is slower than $T^{-1/3}$ and is not simply determined.
[21] W. E. Pickett, Rev. Mod. Phys. **61**, 433 (1989).